Journal of Optoelectronics and Advanced Materials, Vol. 3, No. 4, December 2001, p. 919 - 924

STUDIES AND MAGNETIC PROPERTIES OF Ni-Zn FERRITE SYNTHESIZED FROM THE GLYOXILATES COMPLEX COMBINATION

C. Caizer, M. Stefanescu[a], C. Muntean[a], I. Hrianca

West University of Timisoara, Faculty of Physics, Department of Electricity and Magnetism,
Bd. V. Parvan no.4, 1900-Timisoara, Romania
[a]"Politehnica" University, Faculty of Chemistry and Chemical Engineering, P. Victoriei no.2,
1900-Timisoara, Romania.

In this paper, the influence of temperature and atomic ratio Ni(II):Zn(II):Fe(III) on the forming of the spinel phase $Zn_xFe_{1-x}[Ni_{1-x}Fe_{1+x}]O_4$, (x=0.15; 0.35; 0.50; 0.65; 0.85), obtained from precursors heteropolynuclear complex combination is examined. The samples were analyzed by X-ray diffraction (XRD) which showed that crystalline structure corresponds to the FFC system with the lattice parameter a=0.843 nm in agreement to the Ni-Zn ferrite obtained by other methods and the forming of the ferrite at low temperatures (500 ^{0}C). The differential thermal analysis (DTA) confirmed the spinel phase formation even for the samples heated at 400 ^{0}C, 2 h. The influence of the Zn^{2+} ions concentration on the magnetic quantities of interest (saturation magnetization σ_s, remanent magnetization σ_r, coercive field H_c and magnetic susceptibility χ) was studied. A maximum of the saturation magnetization (σ_s=66.41 emu/g) at x=35 % in agreement with Néel theory was detected.

(Received November 10, 2000; accepted March 6, 2001)

Keywords: Ni-Zn ferrite; Glyoxilate; Zn^{2+} ions; DTA; XRD; Magnetic properties.

1. Introduction

The Ni-Zn ferrite is a spinel with crystalline structure belonging to the cubic system and is generally represented by the following formula: $Zn_xNi_{1-x}Fe_2O_4$, with the molar ratio: $(NiO+ZnO):Fe_2O_3=1$. It is mainly used in high frequency fields as a result of reduced losses. The Ni-Zn ferrite can be obtained by several different methods [1-3], conditioned however by the cost price and by high purity. Particular interest has been dedicated to the methods based on decomposing complex combinations for obtaining ferrite powders with a high degree of dispersion [4-6]. This paper presents the synthesis of the Ni-Zn ferrite. It is done by an adequate thermal treatment of the product mass obtained following the decomposition of hetero-polynuclear complex combinations of the glyoxilate type [7-10]. The complex combinations having the following formula: $Fe_2(Ni,Zn)(OH)_2(C_2H_2O_4)_3 \cdot xH_2O$ are isolated by oxidation in a water solution of the 1,2-ethandiol (ethylenglycol) at glyoxilate dianion ($C_2H_2O_4^{2-}$) of Ni(II), Zn(II), Fe(III) [11]. Practically, the efficiency is 100 %, while the oxidic systems purity depends on the purity of the reagents. There are presented the magnetic properties of the ferrite, the results obtained being discussed within several theoretical developments as well as within the experimental results obtained by other authors.

2. Experimental results and discussions

2.1. Powder ferrite synthesis

During the first stage the complex combination corresponding to the $Ni_{1-x}Zn_xFe_2O_4$ ferrite (x=0.65) has been synthesized . The temperature domain in which the decomposition of the synthesized glyoxilate takes place was established by thermal analysis, making use of a 1500–D Derivatographer (MOM Budapest). Two main processes have been distinguished in the TG, DTG and DTA (Fig. 1) curves: a) loss in the crystallization water up to about 200 °C; b) burning (decomposition) of the ligand together with the elimination of the gaseous products CO, CO_2 having a powerful exothermal effect on the DTA curve, within the temperature interval (200–350) ^{0}C. Within (350–500) °C, the resulting oxidic mass is practically constant. During the second stage, a sufficient quantity of the complex combination has been decomposed at 350 °C, while the resulting product mass, which has magnetic properties, has been subjected to a thermal treatment at 400, 500, 700, 800 and 1000 °C for two hours. The TG and DTA curves are presented in Fig. 2. The recording has been done in the following conditions: sample mass – 1.0 g ; heating speed – 10 °C/minute ; temperature interval – (20 – 1000) °C ; cylindrical crucible of Pt ; medium – static air; reference material - α-Al_2O_3. Studying the reaction of Fe_2O_3 with NiO and with ZnO respectively, in mecanic blends by ATD has shown a strong exothermal effect in the case of Fe_2O_3 + ZnO at 785 °C, and in the case of Fe_2O_3 + NiO an endothermic effect at 790 °C, unaccompanied by weight loss on the TG curve. These effects, also shown by the X-ray diffraction (XRD), have been attributed to the formation of binary ferrites [12]. In our case, the evolution of the curves shows that in the case of the calcinated samples at 400 °C and 500 °C, the mass losses are larger and they are accompanied by weaker exothermal effects at ~ 720 °C, which we attribute to the burning of residual C coming from the organic combination combustion (ligand).

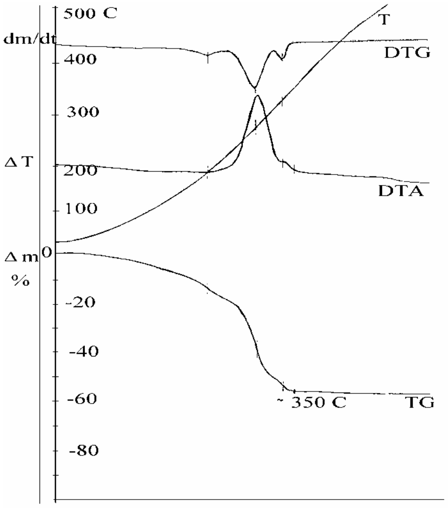

Fig. 1. The derivatogram of the thermal decomposition of the Fe(III)-Ni(II)-Zn(II) glyoxilate.

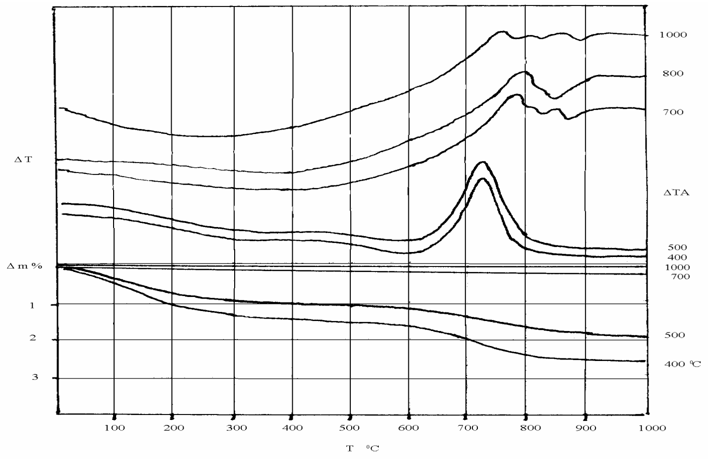

Fig. 2. TG and DTA for samples subject to thermal treatment at 400 ^{o}C, 500 ^{o}C, 700 ^{o}C, 800 ^{O}C and 1000 ^{O}C.

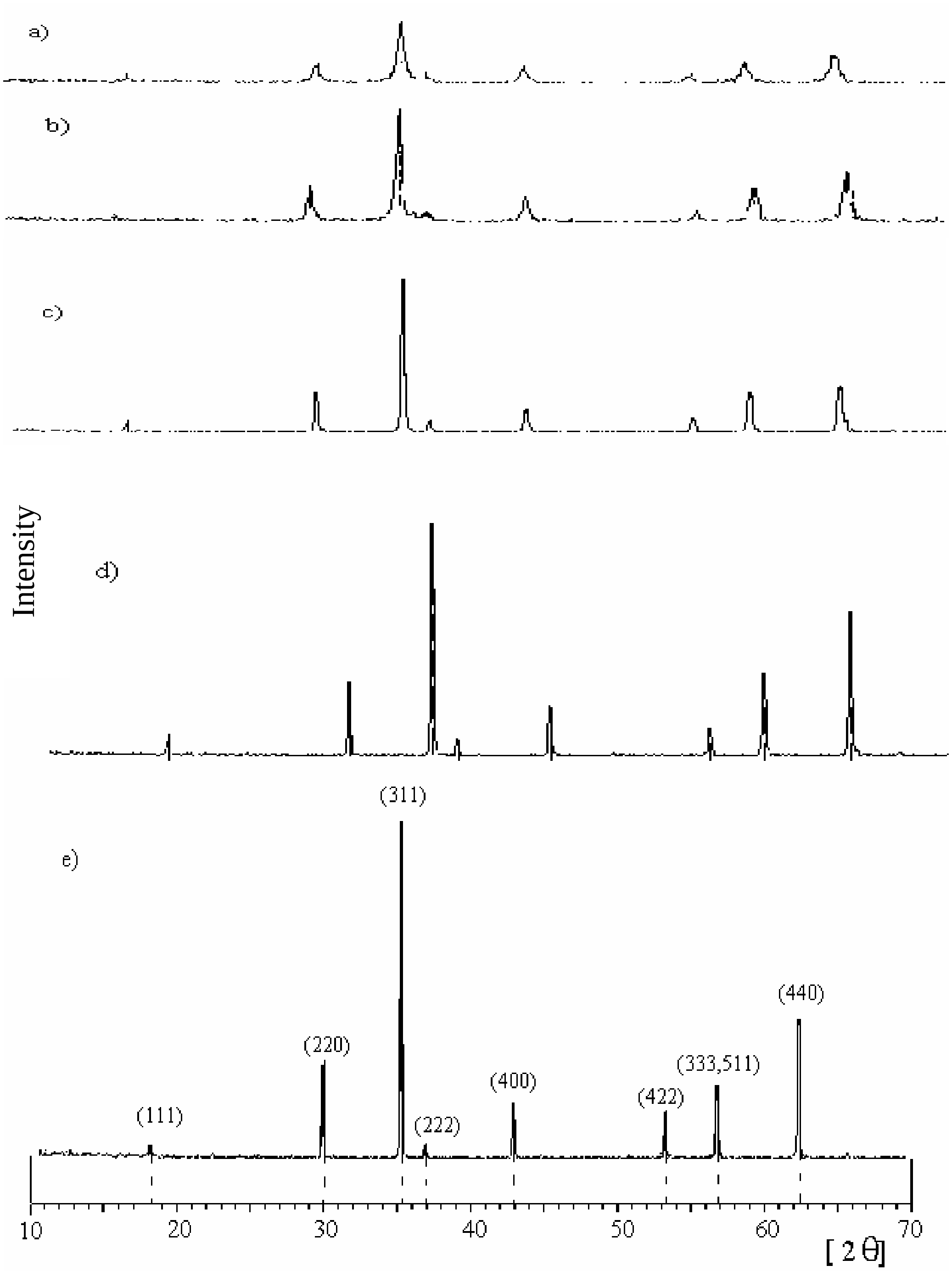

Fig. 3. Diffraction spectra recorded for samples calcinated at 400 ^{0}C (a), 500 ^{0}C (b), 700 ^{0}C (c), 1000 C (d), 1300 ^{0}C (e).

The remaining thermal effects noted in the DTA curbs, with no mass variation, close to 750 °C – 850 °C, are due to the more advanced ordering and formation of the Ni(II)–Zn(II)–Fe(III) spinel. The results let us to conclude that for all samples up to 700 °C there are mixed oxidic systems already formed. In order to clarify these aspects and to identify the formation stages, the samples have also been analyzed by X ray diffraction. The diffraction spectra registered by a PW 3020 Philips diffractometer using the CuKα (λ=1.54056 Å) radiation, have been presented in Fig. 3. For the sample calcinated at 400 ^{0}C, at larger diffraction angles, one can see several diffraction lines close to one another. Having in view the interplanar distances, d, the diffraction angles, 2θ, and distances corresponding to the upper limits, values which correspond to Ni(II) and Zn(II) binary ferrites, we conclude that these compounds: $NiFe_2O_4$, $ZnFe_2O_4$, $(Ni,Zn)Fe_2O_4$, Fe_3O_4, γ-Fe_2O_3 can occur in the system. At 500 ^{0}C there appear lines corresponding to the mixed ferrite in the spectrum and they remain at 700, 800 and 1000 ^{0}C, respectively. The lack of the other upper limits existing at 400 ^{0}C reveals the formation of one and only stage which corresponds to the Ni-Zn mixed ferrite. By calculating the latice constant "a" for the sample calcinated at 1000 ^{0}C, we have obtained a = 0.843 nm, value which corresponds to the Ni-Zn ferrite [13] and it is in agreement with the one published by other authors [14]. The results obtained show the formation of the Ni-Zn ferrite and not the separate stages of $NiFe_2O_4$ and $ZnFe_2O_4$ from the 500 ^{0}C temperature on. Ferrite crystallization is complete at 1000 ^{0}C.

2.2. Magnetic properties

Magnetic measurements, taken with a standard equipment provided with a data acquisition system (DAQ) connected to a computer [11], have been done on the powder sample $Zn_xNi_{1-x}Fe_2O_4$, calcinated at 1000 ^{0}C for 2h, with x = 0,15; 0,35; 0,50; 0,65; 0,85. The registered hysteresis cycles are shown in Fig. 4. In Fig. 5, is shown the variation of the saturation magnetization, σ, as a function of Zn ion concentration.

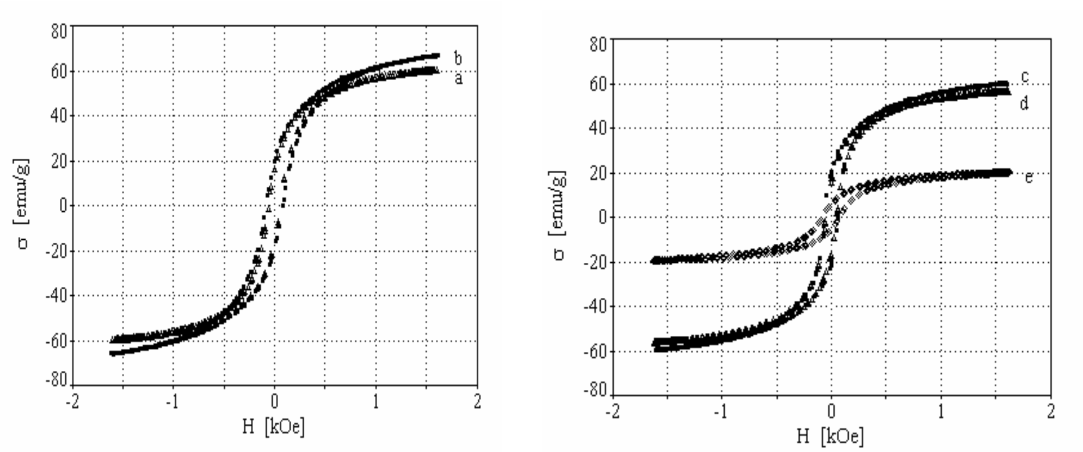

Fig. 4. Hysteresis cycles registered at 50 Hz, for the thermally treated sample at 1000 ^{0}C, 2h, and x = 0.15(a). 0.35(b). 0.50(c). 0.65(d). 0.85(e).

It is obvious that, though Zn^{2+} ions are introduced into the crystalline structure with no magnetic moment, up to x=0.35, yet the saturation magnetization is increasing, reaching the upper limit value σ=66.41 emu/g (Fig. 5). This increase is explained by the change in magnetic ion distribution in the spinelic network of the Ni ferrite where the Fe^{3+} ions (with $5\mu_B$ – Bohr magnetons) are equally distributed in tetrahedral (A) and octahedral (B) positions, while the Ni^{2+} ions (with $2\mu_B$) take octahedral positions exclusively: $Fe^{3+}[Ni^{2+}Fe^{3+}]O_4^{2-}$ (the brackets contain the ions in B positions). The dominant interaction is the one of superchange I_{AB} between the ions in position (A) and (B). Since the Fe^{3+} ions in (A) and (B) positions have equal and opposite magnetic moments, they compensate each other and the complete magnetic moment is exclusively determined by the Ni^{2+} ion. The Zn^{2+} ions introduced in the network are disposed only in tetrahedral positions, dislocating the Fe^{3+} ions, which pass to the octahedral positions: $Zn_x^{2+}Fe_{1-x}^{3+}[Ni_{1-x}^{2+}Fe_{1+x}^{3+}]O_4^{2-}$. In this case the magnetic moments of the Fe^{3+} ions in the two networks (A) and (B) compensate each other no more and due to the bigger magnetic moment of the Fe^{3+} ion the growth in the magnetic moment by molecule (and the saturation magnetization too) is bigger than the increase determined by the diminishing of the number of Ni^{2+} ions. After reaching the x = 0.35 concentration, there takes place a weakening of the I_{AB} superchange interaction, and the parallel orientation of the magnetic moments in the (B) network is altered; two distinct orientations of the magnetic moments appear in the (B) network, that compensate each other only partially [15]. This leads to a progressive decrease of the saturation magnetization reaching the value of 20 emu/g with x = 0.85. When the Ni^{2+} ions are completely replaced, the Fe^{3+} ions in the octahedral network take an antiferromagnetic ordering, which brings about the annulment of the complete magnetic moment by molecule (saturation magnetization included). The result obtained is in agreement with the Néel theoretical development [16] and the experimental results [17, 18]. Table I offers the values of the ratio between σ_r/σ_c and those of the coercitive field H_c, resulting from the hysteresis cycles recorded in the magnetization field H = 1.6 kOe. The reduced values of the σ_r/σ_S ratio (remanent magnetization divided by the saturation magnetization) show a powder ferrite behavior, within the magnetization field, closer to the superparamagnetic one.

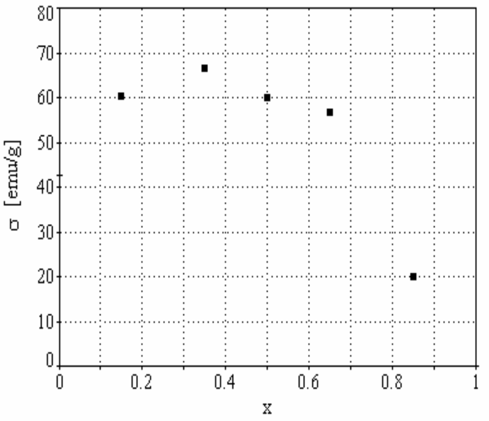

Fig. 5. Saturation magnetization variation with ion concentration for the thermally treated sample at 1000 ^{0}C.

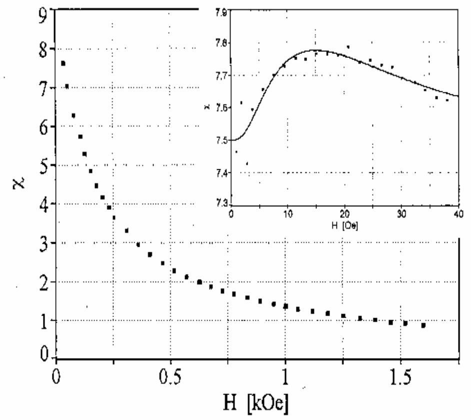

Fig. 6. Magnetic susceptibility to small fields of the powder ferrite after thermal treatment at 1000 ^{o}C, 2 h and x = 0.65.

Table 1. T=1000 ^{0}C, t=2 h

Concentration, x	0.15	0.35	0.50	0.65	0.85
σ_r/σ_S	0.27	0.29	0.33	0.30	0.28
H_c (Oe)	59	79	58	46	75

This behavior is also revealed by the variation of susceptibility (χ) to the magnetic field (Fig. 6). In small fields the magnetic susceptibility presents low values and has a weak upper limit. The values of initial susceptibility χ = 7.5 and upper limit susceptibility χ = 7.78 have been obtained by fitting the experimental points. By calculating the average size of the crystallites using Scherrer's formula [19], we have found the value of 9.0 nm for the sample calcinated at 1000 ^{0}C and x = 0.65. This result indicates that the ferrite nanometrical particles are mono-domain and should behave superparamagnetically. The main causes for deviating from this behavior are: the presence of magnetostatic interactions in the system which lead to the forming of agglomerates (clusters) and the existing distribution according to dimensions of the nanoparticles in the powder [20-21]. In the case of larger particles, which can have a multi-domain structure, movements of the inter-domain Bloch walls accompany the magnetic process. The hysteresis cycles (Fig. 4) show that the magnetization of the system takes place by irreversible processes.

3. Conclusions

Powder (Ni-Zn)Fe_2O_4 ferrite has been obtained from complexes of the glyoxilate type following thermal decomposition at 350 ^{0}C and the calcination of the "residue" obtained in the interval (400 – 1000) ^{0}C. The differential thermal analysis reveals of formation of some mixed oxidic compounds including the (Ni-Zn)Fe_2O_4 ferrite starting at 400 ^{0}C. X-ray diffraction indicates the formation of Ni-Zn ferrite, as single phase, from 500 ^{0}C on. At 1000 ^{0}C the ferrite is well crystallized and has the lattice constant: a = 0.843 nm. The particles in the ferrite powder are nano-metrical in size and the magnetization of the system is not of the superparamagnetic type, due to the magnetostatic interactions and to the particle distribution according to their dimensions. The values registered for the saturation magnetization are in agreement with those published by other authors, for the Ni-Zn ferrite obtained by other methods. The saturation magnetization shows an upper limit (σ=66.41 emu/g) depending on the non-magnetic Zn ion concentration, in perfect accordance to Néel's theory.

References

[1] A. S. Albuquerque, J. D. Ardisson, W. A. A. Macedo, J. Magn. Magn. Mater., **192**, 277 (1999).
[2] R. Valenzuela, *Magnetic ceramics*, Cambridge University Press, Cambridge, (1994).
[3] A. Verma, T. G. Goel, R. G. Mendiratta, R. G. Gupta, J. Magn. Magn. Mater., **192**, 271 (1999).
[4] M. Brezeanu, L. Patron si M. Andruh, *Combinatii complexe polinucleare si aplicatiile lor*, Ed. Acad., Bucuresti, (1986).
[5] M. Barzescu, M. Cristea , M. Stefanescu , Ghe.Constantin, Rom. Pat. 102501, Sept. 27, (1990).
[6] M. A. Verges, M. Martinez , E. Matizevic, J. Mat. Res., **8**, 2916(1993).
[7] M. Birzescu, M. Stefanescu, C. Caizer, M. Stoia, C. Muntean, Prog. Ses. Jub., 29 octomb., Timisoara, (1998).
[8] M. Stefanescu, V. Sasca, V.Levinta, N. Doca, Chem. Bull. T.U.Timisoara, **36**, 60 (1991).
[9] Proceedings of fifth ECERS, Key Eng. Mat, **132-136**, 65 (1997).
[10] M. Stefanescu, V. Sasca, M. Barzescu, J. Therm. Anal., **56**, 579 (1998).
[11] I. Hrianca, C. Caizer, M. Stefanescu, C. Muntean, Prog. 3 rd Conf. Cond. Matt. Phys., Sept. 17- 19 th, Timisoara, Romania, (1999).
[12] I. Zaharescu, M. Balasoiu, M. Sisan, D. Crisan, Rev. Chim., **33**, 447 (1982).
[13] M. Zaharescu, M. Balasoiu, M. Crisan, D. Crisan, Ceramic Powders, 429 (1983).
[14] N. S. Satyamurthy *et. al.*,Phys. Rev., **181**, 969 (1969).
[15] S. Murty *et al.*, Phys. Rev., **181**, 77 (1969).
[16] L. Neel, Ann. Phys, **3**, 137 (1948).
[17] B. Boucher, R. Buhl, M. Perrin, phys. status sol., **40**, 171 (1970).
[18] L. M. Rao, Proc. Fifth Int. Conf. Ferrites, India, (1989), p. 385.
[19] H. P. Klug, L. E. Alexander, *X-Ray Diffraction Procedure*, 2-nd Edition, Wiley and Sons, Inc., New-York, (1974).
[20] M. El-Hilo, R. W. Chantrell, K. O'Grady, J. Appl. Phys, **84**, 5114 (1998).
[21] I. Hrianca, C. Caizer, M. Stefanescu, C. Muntean, Rom. J. Phys., (1999) (accepted).